4. L.-H. Hsieh and K. Chang, High-efficiency piezoelectric-transducer tuned feedback microstrip ring-resonator oscillators operating at high resonant frequencies, IEEE Trans Microwave Theory Tech 51 (2003), pp. 1141–1145.
5. J. Choi, M. Nick, and A. Mortazawi, Low phase-noise planar oscillators employing elliptic-response bandpass filters, IEEE Trans Microwave Theory Tech 57 (2009), pp. 1959–1965.
6. Y.Q. Wang, W. Hong, Y.D. Dong, B. Liu, H.J. Tang, J.X. Chen, X.X. Yin, and K. Wu, Half mode substrate integrated waveguide (HMSIW) bandpass filter, IEEE Microwave Wireless Compon Lett 17 (2007), pp. 265–267.
7. Y. Cassivi and K. Wu, Low cost microwave oscillator using substrate integrated waveguide cavity, IEEE Microwave Wireless Compon Lett 13 (2003), pp. 48–50.
8. J. Nallatamby, M. Prigent, M. Camiade, and J.J. Obregon, Extension of the Leeson formula to phase noise calculation in transistor oscillators with complex tank, IEEE Trans Microwave Theory and Tech MTT-51 (2003), pp. 690–696.

INTERNAL MOBILE PHONE ANTENNA ARRAY FOR LTE/WWAN AND LTE MIMO OPERATIONS

Kin-Lu Wong, Ting-Wei Kang, and Ming-Fang Tu
Department of Electrical Engineering, National Sun Yat-sen University, Kaohsiung 80424, Taiwan; Corresponding author: kangtw@ema.ee.nsysu.edu.tw

Received 22 September 2010

ABSTRACT: *An antenna array comprising a main antenna for eight-band LTE/WWAN operation and an auxiliary antenna to combine with the main antenna for LTE MIMO operation in the mobile phone is presented. Both the main and auxiliary antennas are disposed at the bottom edge of the system circuit board of the mobile phone and separated by a protruded ground. The main and auxiliary antennas can respectively fit in two small no-ground regions of 15 × 30 mm^2 and 15 × 20 mm^2 on the system circuit board, while the protruded ground in-between the two antennas has a width of 10 mm for mounting a USB data port. The main antenna covers the 704–960/1710–2690 MHz bands for eight-band LTE/WWAN operation, and the auxiliary antenna covers the 704–787/2300–2690 MHz bands such that the main and auxiliary antennas together can perform LTE MIMO operation in the LTE700/2300/2500 bands. The proposed antenna array is fabricated and tested. Results are presented and discussed.* © 2011 Wiley Periodicals, Inc.
Microwave Opt Technol Lett 53:1569–1573, 2011; View this article online at wileyonlinelibrary.com. DOI 10.1002/mop.26038

Key words: *mobile antennas; handset antennas; LTE antennas; WWAN antennas; multi-input multi-output operation*

1. INTRODUCTION

Recently, the long-term evolution (LTE) system [1] is introduced to provide better mobile broadband and multimedia services than the existing wireless wide area network (WWAN) mobile networks. Some promising internal antennas for applications in the mobile communication devices including the mobile phones and notebook computers to cover eight-band LTE/WWAN operation in the 704–960/1710–2690 MHz bands have also been demonstrated [2–6]. Further, to achieve a much higher channel capacity over the traditional wireless system with a single antenna [7–11], the MIMO (multi-input multi-output) operation of the LTE system in the LTE700 (704–787 MHz), LTE2300 (2300–2400 MHz) and LTE2500 (2500–2690 MHz) bands is also demanded. For achieving LTE MIMO operation, two or more LTE antennas are required to be used in the mobile communication devices. This causes a design challenge for the internal LTE antennas to be applied in the mobile communication devices, especially in the mobile phones, because of the very limited internal spaces available in the mobile phones for using the internal antennas.

In this article, we present a promising design of a mobile phone antenna array comprising a main antenna for eight-band LTE/WWAN operation and an auxiliary antenna covering three-band LTE700/2300/2500 to perform LTE MIMO operation with the main antenna. Both the main and auxiliary antennas are disposed at the bottom edge of the system circuit board of the mobile phone and separated by a protruded ground, which can accommodate a universal serial bus (USB) connector [12] as the data port for the mobile phone. Note that with the internal WWAN antennas mounted at the bottom edge of the mobile phone, decreased SAR (specific absorption rate) values to meet the limit of 1.6 W/kg for 1-g head tissue [13] for practical applications can be obtained for the mobile phone [14–17].

The main and auxiliary antennas are both in the form of a coupled-fed loop antenna connected with a chip-inductor-loaded strip [18]. The antenna's upper band is contributed by the coupled-fed loop antenna operated at its 0.5-wavelength resonant mode, while the lower band is mainly owing to the chip-inductor-loaded strip connected to the coupled-fed loop antenna to form a coupled-fed shorted monopole antenna operated at its 0.25-wavelength resonant mode. In addition, such internal mobile phone antennas can be in compact integration with nearby system ground plane on the system circuit board. With this advantageous feature, the main and auxiliary antennas obtained based on this kind of internal mobile phone antenna can respectively fit in two small no-ground regions of 15 × 30 mm^2 and 15 × 20 mm^2 at the bottom edge of the system circuit board and also separated by a protruded ground for accommodating a USB data port. The proposed antenna array is fabricated and tested. Experimental and simulation results of the fabricated antenna array are presented and analyzed.

2. PROPOSED ANTENNA ARRAY

Figure 1(a) shows the configuration of the proposed internal mobile phone antenna array comprising a main antenna and an auxiliary antenna. The antenna array is mounted at the bottom edge of the mobile phone and their detailed dimensions are given in Figure 1(b). A plastic casing with relative permittivity 3.0 and loss tangent 0.02 to simulate a practical mobile phone casing is also included in the study. The proposed antenna array was also fabricated and tested, and the photo of the fabricated antenna array is shown in Figure 2. Note that a practical USB connector is added on the protruded ground in-between the two antennas.

Both the main and auxiliary antennas apply the design technique of the coupled-fed loop antenna connected with a chip-inductor-loaded strip [18] to achieve two wide operating bands with a small size. The main antenna is disposed on a no-ground board space of 30 × 15 mm^2 at one of the corners of the bottom edge. The feeding point at point A_1 is considered as Port 1 in the antenna array. Point B_1 is the shorting point of the coupled-fed loop antenna in the main antenna, which contributes a 0.5-wavelength loop resonant mode [19–21] to form a wide upper band covering the GSM1800/1900/UMTS/LTE2300/2500 (1710–2690 MHz) operation. At point C_1, the chip-inductor-loaded strip is connected to the coupled-fed loop antenna to form a coupled-fed shorted monopole antenna which contributes a wide lower band to cover the LTE700/GSM850/900 (704–960 MHz) operation. The chip inductor used in the main antenna has an inductance of 8.2 nH (L_1), which compensates for the

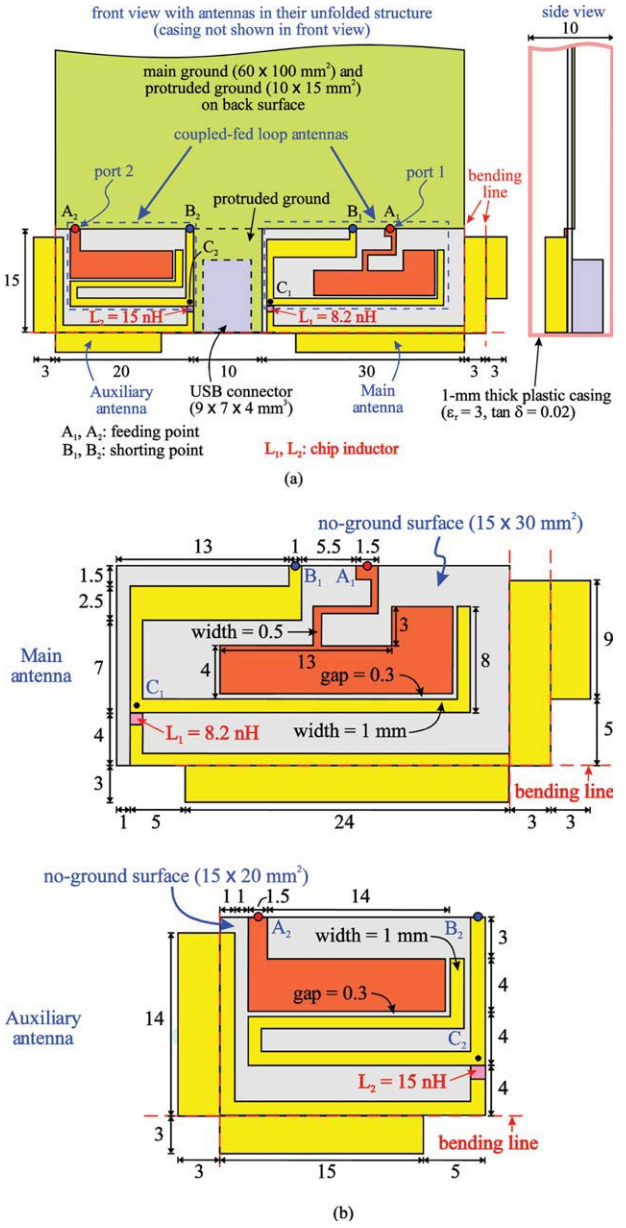

Figure 1 (a) Configuration of the internal mobile phone antenna array comprising a main antenna for eight-band LTE/WWAN operation and an auxiliary antenna to perform LTE MIMO operation with the main antenna. The antenna array is mounted at the bottom edge of the mobile phone. (b) Dimensions of the main and auxiliary antennas. [Color figure can be viewed in the online issue, which is available at wileyonlinelibrary.com]

increased capacitance with decreasing resonant length of the monopole antenna and thus effectively decreases the required length for generating the 0.25-wavelength monopole resonant mode [22–27]. The widened end section of the chip-inductor-loaded strip is for widening the lower-band bandwidth of the main antenna. The operating principle of the antenna has been discussed in [18]. However, the obtained lower-band bandwidth for the main antenna is wider than that obtained in Ref. 18, in which the lower-band bandwidth can cover only the GSM850/900 (824–960 MHz) operation.

The auxiliary antenna requires a smaller no-ground board space of 15 × 20 mm^2 and can provide a lower band for covering the LTE700 (704–787 MHz) operation and an upper band for covering the LTE2300/2500 (2300–2690 MHz) operation. The upper band is contributed by the coupled-fed loop antenna in the auxiliary antenna, with point A_2 as the feeding point and point B_2 as the shorting point. Point A_2 is considered as Port 2 in the antenna array. Similar to the main antenna, the lower band is contributed by the chip-inductor-loaded strip connected to the coupled-fed loop antenna at point C_2. The chip inductor with an inductance of 15 nH (L_2) is used in the auxiliary antenna. This chip inductor also leads to a smaller strip length required for generating a 0.25-wavelength monopole resonant mode at about 700 MHz for the lower band of the auxiliary antenna.

Note that the protruded ground of size 10 × 15 mm^2 in-between the main and auxiliary antennas not only can be used for accommodating a USB connector of size 9 × 7 × 4 mm^3 (see the photo of the fabricated antenna in Figure 2, which is usually located at the bottom edge of the mobile phone, but also can enhance the isolation between the main and auxiliary antennas. With enhanced isolation, better envelope or pattern correlation coefficient ρ_e computed from the S parameters as shown in Eq. (1) [28] can be obtained.

$$\rho_e = \frac{\left|S_{11}^* S_{12} + S_{21}^* S_{22}\right|^2}{\left[1 - \left(|S_{11}|^2 + |S_{21}|^2\right)\right]\left[1 - \left(|S_{22}|^2 + |S_{12}|^2\right)\right]} \quad (1)$$

The obtained correlation coefficient ρ_e is less than 0.12 over the LTE700/2300/2500 bands between Port 1 and 2 in the proposed design, which is acceptable for MIMO applications [29, 30]. Detailed results are discussed in Section 3.

3. RESULTS AND DISCUSSION

Figure 3 shows the measured and simulated S parameters (S_{11}, S_{21}, S_{22}) for the fabricated antenna array shown in Figure 2. For the measurement of the main antenna, it is excited with the auxiliary antenna terminated to 50 Ω, and vice versa for the auxiliary antenna, which is excited with the main antenna terminated to 50 Ω. The simulated results are obtained using simulation software high frequency structure simulator (HFSS) [31]. The measured data of the S parameters agree with the simulated results. From the S_{11} results, the bandwidth of the main antenna covers the desired 704–960 and 1710–2690 MHz bands for eight-band LTE/WWAN operation. Although from the S_{22}

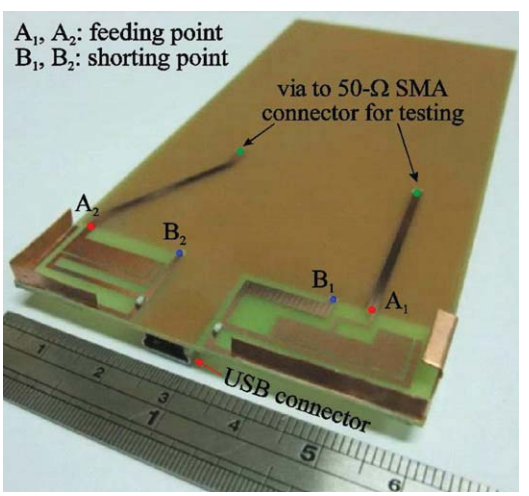

Figure 2 Photo of the fabricated antenna array (mobile phone casing not included in the photo). (a) Measured and (b) simulated S parameters (S_{11}, S_{21}, S_{22}) for the proposed antenna array. The main (auxiliary) antenna is excited with the auxiliary (main) antenna terminated to 50 Ω. [Color figure can be viewed in the online issue, which is available at wileyonlinelibrary.com]

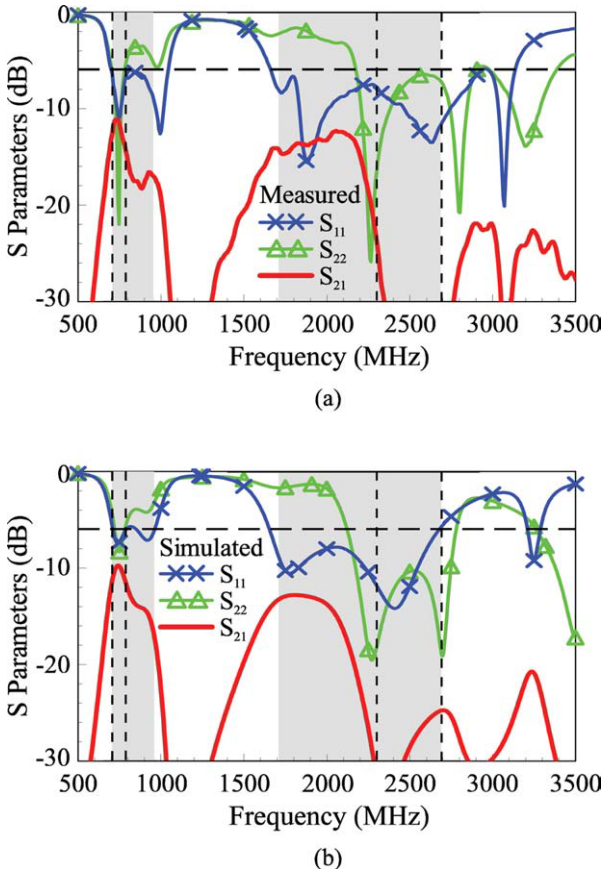

Figure 3 (a) Measured and (b) simulated S Parameters (S_{11}, S_{21}, S_{22}) for the proposed antena array. The main (auxiliary) antena is excited with the auxiliary (main) antena terminated to 50 Ω. [Color figure can be viewed in the online issue, which is available at wileyonlinelibrary.com]

results, the bandwidth of the auxiliary antenna covers three-band LTE (704–787/2300–2690 MHz) operation. The measured isolation (S_{22}) between the main and auxiliary antennas for LTE MIMO operation in the LTE700 and LTE2300/2500 bands is less than about −11 dB and −22 dB, respectively. From the measured S parameters, the envelope correlation coefficient ρ_e is computed and shown in Figure 4. Over the LTE700 band, the maximum coefficient ρ_e is 0.12 only. On the other hand, over the LTE2300/2500 bands, very small coefficient ρ_e is obtained, which is nearly zero. The obtained envelope correlation coefficient indicates that the proposed antenna array is promising for LTE MIMO operation.

Figure 5 shows the measured three-dimensional total-power radiation patterns at 750, 1940, and 2500 MHz for the main

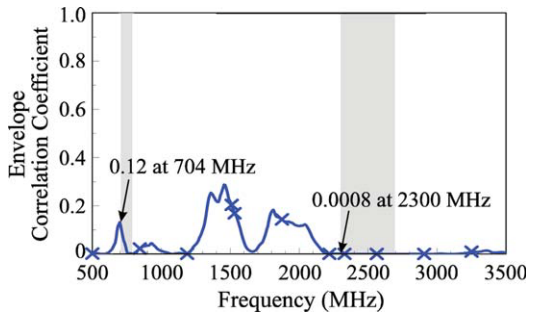

Figure 4 Envelope correlation coefficient ρ_e obtained from the measured S parameters in Figure 3. [Color figure can be viewed in the online issue, which is available at wileyonlinelibrary.com]

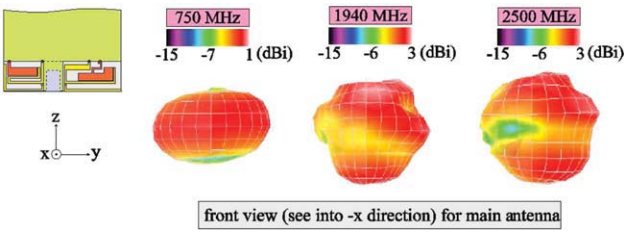

Figure 5 Measured three-dimensional total-power radiation patterns for the main antenna. [Color figure can be viewed in the online issue, which is available at wileyonlinelibrary.com]

antenna. The measurement is conducted in a far-field anechoic chamber. At 750 MHz in the lower band, dipole-like radiation pattern is seen. Although at 1940 and 2500 MHz in the upper band, more variations in the radiation patterns are observed. The measured radiation patterns are similar to those of the reported internal WWAN or LTE/WWAN mobile phone antennas [3–6], and there are no special distinctions. The measured radiation patterns at 750 and 2500 MHz for the auxiliary antenna are shown in Figure 6. Similar characteristics of the radiation patterns for frequencies in the lower and upper bands as those for the main antenna are observed.

The measured antenna efficiency including the mismatching loss for the main antenna is presented in Figure 7. Over the lower band (704–960 MHz) and upper band (1710–2690 MHz), the antenna efficiencies are about 48–60% and 63–82%, respectively. For the auxiliary antenna (results shown in Fig. 8), the antenna efficiency in the lower band (704–787 MHz) and upper band (2300–2690 MHz) are, respetcively, about 42–48% and 50–70%. The obtained antenna efficiencies over the operating bands are reasonable for practcial mobile phone applications.

Finally, the S parameters for the cases of the main and auxiliary antennas mounted at opposite edges of the system circuit board are studied. Two cases are analyzed. The first case is for the two antennas located at diagonal corners of the system circuit board as shown in Case A in the figure. The second case is for the two antennas located at adjacent corners as shown in Case B in the figure. Similar as the proposed design studied in Figure 3, the obtained S_{11} and S_{22} results for the two antennas cover the desired operating bands. However, from the S_{21} results, Case A and B show degraded isolation between the two antennas in both the lower and upper bands as compared to those obtained for the proposed design in Figure 3. This behavior can be attributed to the reason that the system ground plane on the system circuit board is also an efficient radiator for the mobile phone, especially in the lower band [32–34], and the antenna performances are greatly dependent on the length of the system ground plane. Hence, when the main antenna is excited at the bottom edge, there are still strong excited surface currents

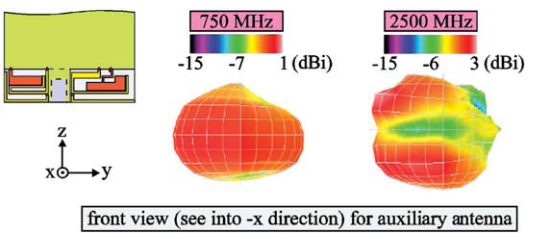

Figure 6 Measured three-dimensional total-power radiation patterns for the auxiliary antenna. [Color figure can be viewed in the online issue, which is available at wileyonlinelibrary.com]

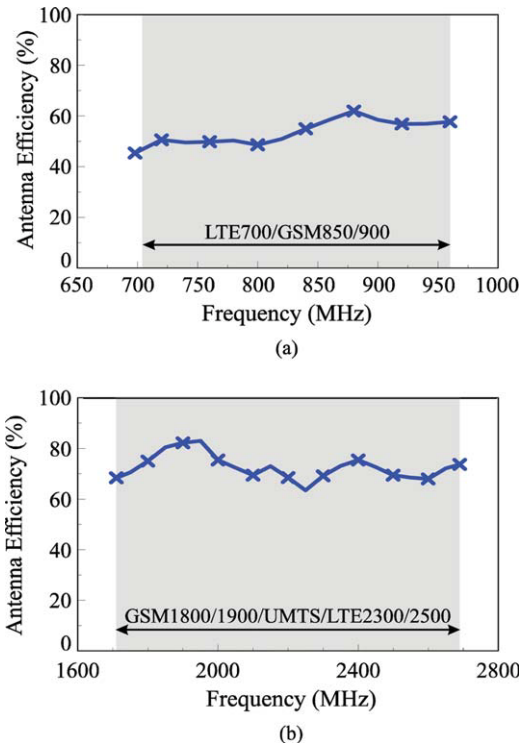

Figure 7 Measured antenna efficiency (mismatching loss included) for the main antenna. (a) The lower band (704–960 MHz). (b) The upper band (1710–2690 MHz). [Color figure can be viewed in the online issue, which is available at wileyonlinelibrary.com]

at the top edge of the system ground plane, which leads to degraded isolation between the two antennas. On the other hand, although the two antennas show a small distance in-between in the proposed design, better isolation can be obtained. This is because the shorter edge or the bottom edge of the system ground plane is not at resonance, and hence acceptable isolation between the two antennas in the proposed design can be achieved. From the obtained results, the proposed design for the two antennas located at the same edge (bottom edge here) of the system circuit board is most promising for practical mobile phone applications.

4. CONCLUSIONS

An internal mobile phone antenna array for LTE/WWAN and LTE MIMO operations has been proposed. The antenna array comprises a main antenna and an auxiliary antenna, both showing small size and suitable to be disposed at the bottom edge of the system circuit board of the mobile phone. The main antenna can cover eight-band LTE/WWAN operation, while the auxiliary antenna can cover three-band LTE operation. In-between the two antennas, a USB connector can also be mounted to serve as the data port of the mobile phone, leading to compact integration of the proposed antenna array inside the mobile phone. Good radiation characteristics of the two antennas have also been observed. Acceptable isolation and envelope correlation coefficient between the main and auxiliary antennas have been obtained, which makes it promising for the main and auxiliary antennas to perform LTE MIMO operation over the LTE700/2300/2500 bands.

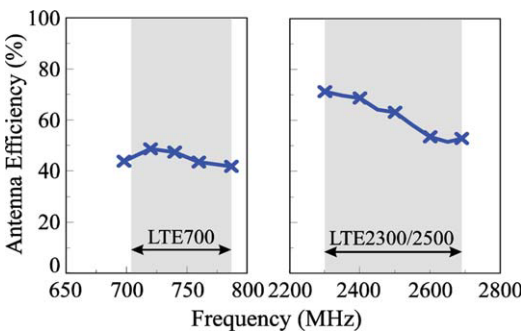

Figure 8 Measured antenna efficiency (mismatching loss included) in the lower band (704–787 MHz) and upper band (2300–2690 MHz) for the auxiliary antenna. [Color figure can be viewed in the online issue, which is available at wileyonlinelibrary.com]

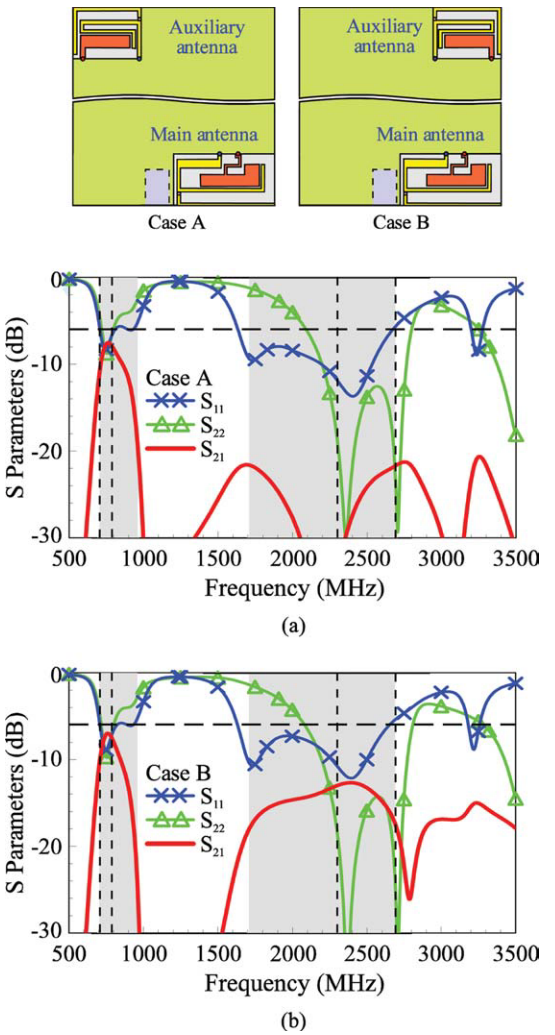

Figure 9 Simulated *S* parameters for the main and auxiliary antennas mounted at opposite edges of the mobile phone. (a) Case A (the two antennas located at diagonal corners). (b) Case B (the two antennas located at adjacent corners). [Color figure can be viewed in the online issue, which is available at wileyonlinelibrary.com]

REFERENCES

1. Available at: http://en.wikipedia.org/wiki/3GPP_Long_Term_Evolution, Wikipedia, the free encyclopedia: 3GPP Long Term Evolution.
2. T.W. Kang and K.L. Wong, Internal printed loop/monopole combo antenna for LTE/GSM/UMTS operation in the laptop computer, Microwave Opt Technol Lett 52 (2010), 1673–1678.

3. C.T. Lee and K.L. Wong, Planar monopole with a coupling feed and an inductive shorting strip for LTE/GSM/UMTS operation in the mobile phone, IEEE Trans Antennas Propag 58 (2010), 2479–2483.
4. K.L. Wong, M.F. Tu, C.Y. Wu, and W.Y. Li, Small-size coupled-fed printed PIFA for internal eight-band LTE/GSM/UMTS mobile phone antenna, Microwave Opt Technol Lett 52 (2010), 2123–2128.
5. S.C. Chen and K.L. Wong, Bandwidth enhancement of coupled-fed on-board printed PIFA using bypass radiating strip for eight-band LTE/GSM/UMTS slim mobile phone, Microwave Opt Technol Lett 52 (2010), 2059–2065.
6. K.L. Wong, W.Y. Chen, C.Y. Wu, and W.Y. Li, Small-size internal eight-band LTE/WWAN mobile phone antenna with internal distributed LC matching circuit, Microwave Opt Technol Lett 52 (2010), 2244–2250.
7. Multiple-input multiple-output, Wikipedia, Available at: http://en.wikipedia.org/wiki/MIMO.
8. K.L. Wong, C.H. Chang, B. Chen, and S. Yang, Three-antenna MIMO system for WLAN operation in a PDA phone, Microwave Opt Technol Lett 48 (2006), 1238–1242.
9. K.L. Wong and J.H. Chou, Printed collinear two-antenna element for WLAN access points in a MIMO system, Microwave Opt Technol Lett 48 (2006), 930–933.
10. V. Plicanic, B.K. Lau, A. Derneryd, and Z. Ying, Actual diversity performance of a multiband diversity antenna with hand and head effects, IEEE Trans Antennas Propag 57 (2009), 1547–1556.
11. R.A. Bhatti, J.H. Choi, and S.O. Park, Quad-band MIMO antenna array for portable wireless communications terminals, IEEE Antennas Wirel Propag Lett 8 (2009), 129–132.
12. Available at: http://en.wikipedia.org/wiki/Universal_Serial_Bus, Wikipedia, the free encyclopedia: Universal Serial Bus.
13. American National Standards Institute (ANSI), Safety levels with respect to human exposure to radio-frequency electromagnetic field, 3 kHz to 300 GHz, ANSI/IEEE standard C95.1, 1999.
14. C.H. Chang and K.L. Wong, Printed λ/8-PIFA for penta-band WWAN operation in the mobile phone, IEEE Trans Antennas Propag 57 (2009), 1373–1381.
15. C.H. Li, E. Ofli, N. Chavannes, and N. Kuster, Effects of hand phantom on mobile phone antenna performance, IEEE Trans Antennas Propag 57 (2009), 2763–2770.
16. Y.W. Chi and K.L. Wong, Quarter-wavelength printed loop antenna with an internal printed matching circuit for GSM/DCS/PCS/UMTS operation in the mobile phone, IEEE Trans Antennas Propag 57 (2009), 2541–2547.
17. C.T. Lee and K.L. Wong, Internal WWAN clamshell mobile phone antenna using a current trap for reduced groundplane effects, IEEE Trans Antennas Propag 57 (2009), 3303–3308.
18. K.L. Wong, M.F. Tu, C.Y. Wu, and W.Y. Li, On-board 7-band WWAN/LTE antenna with small size and compact integration with nearby ground plane in the mobile phone, Microwave Opt Technol Lett 52 (2010), 2847–2853.
19. Y.W. Chi and K.L. Wong, Quarter-wavelength printed loop antenna with an internal printed matching circuit for GSM/DCS/PCS/UMTS operation in the mobile phone, IEEE Trans Antennas Propag 57 (2009), 2541–2547.
20. Y.W. Chi and K.L. Wong, Very-small-size printed loop antenna for GSM/DCS/PCS/ UMTS operation in the mobile phone, Microwave Opt Technol Lett 51 (2009), 184–192.
21. K.L. Wong and W.Y. Chen, Small-size printed loop antenna for penta-band thin-profile mobile phone application, Microwave Opt Technol Lett 51 (2009), 1512–1517.
22. J. Carr, Antenna toolkit, 2nd ed., Newnes, Oxford, UK., 2001, pp. 111–112.
23. J. Thaysen and K.B. Jakobsen, A size reduction technique for mobile phone PIFA antennas using lumped inductors, Microwave J 48 (2005), 114–126.
24. T.W. Kang and K.L. Wong, Chip-inductor-embedded small-size printed strip monopole for WWAN operation in the mobile phone, Microwave Opt Technol Lett 51 (2009), 966–971.
25. C.H. Chang and K.L. Wong, Small-size printed monopole with a printed distributed inductor for penta-band WWAN mobile phone application, Microwave Opt Technol Lett 51 (2009), 2903–2908.
26. K.L. Wong and S.C. Chen, Printed single-strip monopole using a chip inductor for penta-band WWAN operation in the mobile phone, IEEE Trans Antennas Propag 58 (2010), 1011–1014.
27. C.H. Chang and K.L. Wong, Bandwidth enhancement of internal WWAN antenna using an inductively coupled plate in the small-size mobile phone, Microwave Opt Technol Lett 52 (2010), 1247–1253.
28. S. Blanch, J. Romeu and I. Corbella, Exact representation of antenna system diversity performance from input parameter description, Electron Lett 39 (2003), 705–707, 2003.
29. F.M. Caimi and M. Mongomery, Dual feed, single element antenna for WiMAX MIMO application, Int J Antennas Propag 2008, Article ID 219838.
30. M. Karaboikis, C. Soras, G. Tsachtsiris, and V. Makios, Compact dual-printed inverted-F antenna diversity systems for portable wireless devices, IEEE Antennas Wirel Propag Lett 3 (2004), 9–14.
31. Available at: http://www.ansoft.com/products/hf/hfss/, Ansoft Corporation HFSS.
32. P. Vainikainen, J. Ollikainen, O. Kivekas, and I. Kelander, Resonator-based analysis of the combination of mobile handset antenna and chassis, IEEE Trans Antennas Propag 50 (2002), 1433–1444.
33. J. Villanen, J. Ollikainen, O. Kivekas, and P. Vainikainen, Compact antenna structures for mobile handsets, IEEE 58th Vehicular Technology Conference (VTC-2003-Fall) 1 (2003), 40–44.
34. K.L. Wong and L.C. Lee, Bandwidth enhancement of small-size internal WWAN laptop computer antenna using a resonant open slot embedded in the ground plane, Microwave Opt Technol Lett 52 (2010), 1137–1142.

SIMPLE METHOD TO DESIGN A TRI-BAND BANDPASS FILTER USING ASYMMETRIC SIRs FOR GSM, WiMAX, AND WLAN APPLICATIONS

Wei-Yu Chen,[1] Yi-Hsin Su,[2] Hon Kuan,[2] and Shoou-Jinn Chang[1]
[1] Institute of Microelectronics and Department of Electrical Engineering, Advanced Optoelectronic Technology Center, Center for Micro/Nano Science and Technology, National Cheng Kung University, Taiwan; Corresponding author: mark00.chen@gmail.com
[2] Department of Technology Electro-Optical Engineering, Southern Taiwan University, Taiwan

Received 23 September 2010

ABSTRACT: *This paper presents a simple method to design a tri-band bandpass filter (BPF) using asymmetric stepped-impedance resonators (SIRs) with one-step discontinuity. Only two SIRs are needed in the filter structure. The tri-band passband responses can be achieved by properly selecting the length ratio (*u*) and the impedance ratio (*R*) of the asymmetric SIRs. The performances can be further well tuned by the lengths of two enhanced coupling structure and gap of two asymmetric SIRs. A filter example for the applications of GSM at 1.8 GHz, WiMAX at 3.5 GHz and WLAN at 5.2 GHz was designed and fabricated. The measured results are in good agreement with the full-wave simulation results.* © 2011 Wiley Periodicals, Inc. Microwave Opt Technol Lett 53:1573–1576, 2011; View this article online at wileyonlinelibrary.com. DOI 10.1002/mop.26037

Key words: *tri-band; bandpass filter; stepped impedance resonator*

1. INTRODUCTION

Recently, the development of multiservice wireless system and mobile communication system are attractive in academic